

天然气管道在役焊接径向变形数值模拟

郭广飞^{1,2}, 王 勇², 韩 涛²

(1. 中国石油大学(华东)机电工程学院, 青岛 266580;

2. 合肥通用机械研究院 国家压力容器与管道安全工程技术研究中心, 合肥 230031)

摘 要: 采用焊接模拟软件 SYSWELD 研究了压力及修复时间对天然气管道在役焊接径向变形的影响, 并进行了试验验证。结果表明, 在 0~4 MPa 压力范围内, 径向变形量随压力的增大而增大, 在 4~6 MPa 压力范围内, 径向变形随着压力的增大而减小, 并在 6 MPa 压力时近似等于常压焊接的变形量; 随着焊接修复时间的增加, 径向变形量逐渐增大, 具有时间效应; 预测焊接烧穿时, 瞬时径向最大变形法优于内部点径向变形法。

关键词: 在役焊接; 天然气管线; 径向变形; 数值模拟

中图分类号: TG 402 **文献标识码:** A **文章编号:** 0253-360X(2014)12-0055-04

0 序 言

天然气管道在使用过程中随着腐蚀等因素的影响, 局部减薄, 需要进行修复^[1,2], 而在役焊接具有不停输带压修复的特点, 可保证管道输送的连续性, 避免管道停输进行修复所带来的损失^[3,4], 所以在役焊接技术在天然气管道修复方面具有良好的实用意义。随着焊接电弧热使得焊接处的承载能力下降到一定程度时^[5], 会发生烧穿失稳, 带来严重的安全问题^[6], 所以防止烧穿是在役焊接修复所要考虑的首要问题。在役焊接时, 管道受到内部压力以及焊接应力的共同作用, 其中力的作用使得被焊接管道发生一定量的径向变形, 而焊接热输入使得被焊接管道的强度逐步降低^[7], 促进了径向变形量的增大, 当变形量超过被焊接板厚的 0.1 倍时^[8], 极易发生烧穿, 这为从研究径向变形的角度去研究在役焊接烧穿创造了条件。文中从管道在焊接修复过程中的径向变形着手, 采用焊接模拟软件 SYSWELD 模拟计算并结合试验研究, 探讨压力以及修复时间对在役焊接径向变形(定义其为 U_r) 的影响, 从而研究这些因素对烧穿的影响。

1 在役焊接数值模型的建立

1.1 几何模型

在 SYSWELD 自带的 Visual-Mesh 软件下建模,

SYSWELD 进行计算, 采用图 1 所示的圆周焊缝进行修复, 焊道分布及顺序如图 2 所示。

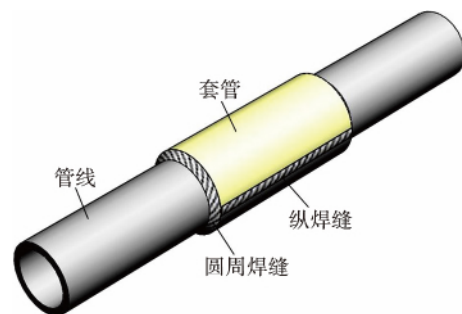


图 1 天然气管道在役焊接修复示意图

Fig. 1 Sketch map of in-service welding pipeline

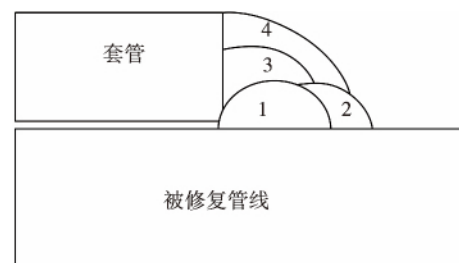


图 2 焊接接头示意图

Fig. 2 Sketch map of welded joint

烧穿一般先发生于 1 焊道焊缝, 所以对焊接接头的第一道焊接时管道内壁的径向变形进行研究。

鉴于第一道焊缝对于被修管线的焊接属于表面堆焊, 采用图 3a 所用的有限元模型, 并且由于管道

收稿日期: 2013-05-27

基金项目: 国家自然科学基金(51074174)及山东省自然科学基金(ZR2010EM041)资助项目

是轴对称的,采用二分之一模型,并且焊缝区的网格较密,这样在减少计算量的同时,也能得到较好的计算精度.天然气管道壁厚为 4.5 mm,管道外径 508 mm,管道宽度取为 200 mm,如图 3 所示.

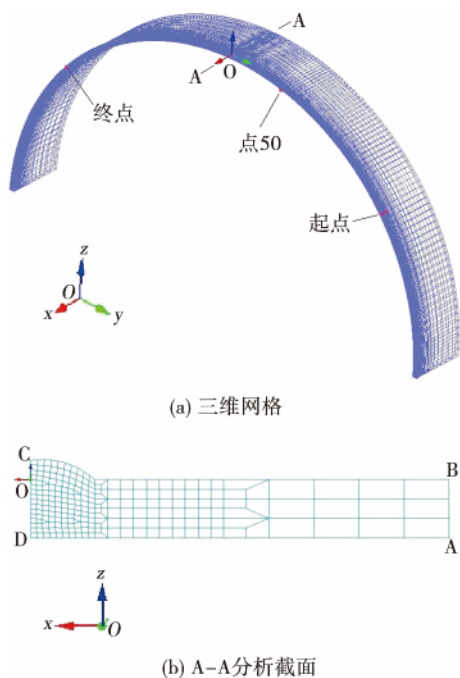


图 3 有限元模型

Fig. 3 Finite element model

1.2 换热边界条件和力学约束

管道外表面和空气的换热主要考虑热辐射换热以及空气的自然对流换热^[7-12],总换热系数为式(1)所示,接头背面与管道内部介质为管内强迫对流换热,换热系数如式(2)所示.

$$\alpha = 4.536 \times 10^{-8} (546.3 + T_0 + T)$$

$$[(273.15 + T_0)^2 + (273.15 + T)^2] + 25 \quad (1)$$

式中: T_0 , T 分别为环境温度(文中为 20 °C)和焊接接头与空气接触表面的温度(°C).

$$\alpha_1 = 0.027 \frac{\lambda}{d} Re^{0.8} Pr^{1/3} \left(\frac{\mu}{\mu_w} \right)^{0.14} \quad (2)$$

式中: λ , Re , Pr , μ 分别为水的导热系数、雷诺数、普朗特数、动力粘度; d 为管道内径; μ_w 为水在壁温时的动力粘度.

模型两端的力学约束为刚性约束,管道材料 X70 管线钢的导热系数和比热容采用文献[10]的公式计算.

天然气的换热系数随着压力的不同,发生着变化,计算中,对不同压力对 α_1 进行相应调整.天然气中甲烷占绝大多数,试验内部天然气换热系数采用甲烷的代替,并且参照文献[11]的数据进行确定.

2 计算结果分析与讨论

2.1 不同压力对径向变形量的影响

采用 SYSWELD 模拟软件针对在役焊接修复过程进行模拟计算,得到各压力工况下 150 s 各时刻变形场,然后运用软件自带的后处理模块得到各时刻最大瞬时径向变形量 $U_{r_{\max}}$,再进行数据处理,得到图 4 所示的计算结果.

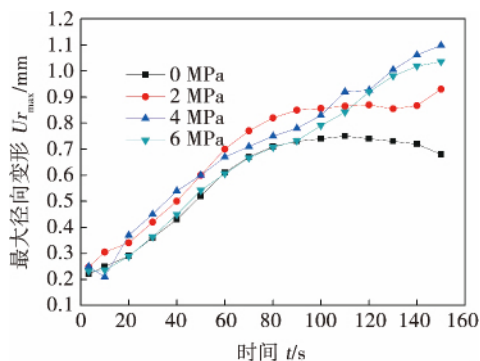


图 4 不同压力下的径向变形量

Fig. 4 Radial direction deformation of different pressure

从图 4 可见,在焊接修复前 50 s 内,在 0 ~ 4 MPa 压力范围内, $U_{r_{\max}}$ 总体上是随着压力的增加而增大,在 4 ~ 6 MPa 范围内, $U_{r_{\max}}$ 随着压力的增大而出现了减小的趋势.通过研究各压力下的换热系数可知,随着压力的增大,管道内的天然气的密度也逐渐增大,此外,压力的增大也带来了管道内部气体流速的增大,这些因素使得天然气的换热能力得到了较大的增大,但是在 0 ~ 4 MPa 范围内,换热系数的增大并不能抵消压力增大对径向变形增大的贡献值,这就是 0 ~ 4 MPa 内随着压力的增大,径向变形量也随之增大的原因;而在 4 ~ 6 MPa 内,换热系数以及天然气流速的增大带来的换热能力的增大,使得可以削弱压力对径向变形的影响.并且从图 4 中可以见到 6 MPa 压力下,在焊接进行的前 90 s 内,和 0 MPa 也就是常压下焊接修复的 $U_{r_{\max}}$ 变化情形类似,所以在以下内容将以 6 MPa 压力下的变形情况为例进行阐述.

2.2 最大径向变形量的时间效应

在内压 6 MPa 下,采用表 1 中提供的焊接参数进行数值模拟并结合试验,考察最大径向变形量 $U_{r_{\max}}$ 随时间变化的情况,如图 5.

在 6 MPa 内压下,在修复之前,管道已经出现了约为 0.2 mm 的径向变形量,随着焊接时间的延长,径向变形量也逐渐变大.这是由于随着热作用的时



图 5 烧穿形貌图

Fig. 5 Macrograph of burnthrough

间增加,被焊管道性能下降的程度越来越大,承压能力逐渐降低。

在之前的焊接变形计算中,没有考虑焊接时间对焊接修复变形的影响,认为如果只要径向变形量 U_r 与板厚 B 的比值小于 0.1,就不会发生烧穿^[8],而计算结果表明,在焊接修复过程中,在焊接进行到一定时间,发生了烧穿,这就表明了焊接修复时间是有限制的,这也就是说在一定焊接速度下单次焊道长度是有限制的,而试验也验证了计算结果,如图 5 所示。

从图 5 可见,在给定的焊接参数条件下,焊接前段并没有产生烧穿,通常认为这些焊接参数是安全的,而计算结果以及试验表明,这样的判断是不严谨的,实际焊接修复中在严格遵守给定焊接参数的情况下,还要严格限制连续焊接的焊道长度,尽量采用中短焊缝,不宜采用长焊缝连续焊接修复。

从图 4 计算结果中也可以研判,在焊接修复进行到 50 s 时,各压力情况下的径向变形量都已经达到了甚至超过了 0.45 mm,也就是板厚的 0.1 倍,这也是发生烧穿的临界径向变形量,而在实际焊接修复试验中,也已经发生了烧穿,验证了计算结果。

将烧穿部位进行切割,选取烧穿临近部位 A 区,观察径向变形,如图 6 所示。从中可知,其总体径向变形量约为 0.5 mm 变形,与计算结果基本吻合。在下面的讨论中将研究焊接进行到 50 s 时板正下方内壁一点 50(图 3a)的径向变形情况。

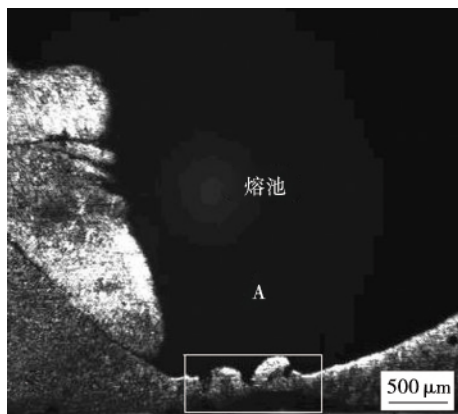


图 6 焊接烧穿临近区域断口

Fig. 6 Cross-sectional macrograph close to burnthrough zone

2.3 50 s 时内部点径向变形量

考察焊接进行到 50 s 时时 A-A 截面下方点 50(图 3a)点的瞬时径向变形量的变化情况,结果如图 7 所示。

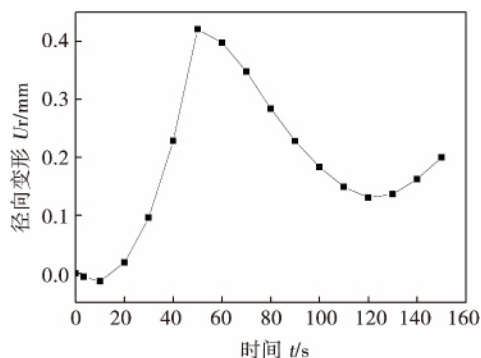


图 7 径向变形示意图

Fig. 7 Sketch map of radial direction deformation

焊接起始阶段,变形内凹,随着焊接过程进行,在第 10 s 时内凹变形达到最大值,之后随着焊接的进行,在第 15 s 时,径向变形开始转变为外凸变形,与之前研究相符^[13],并随着热源逐渐接近点 50,径向变形量也逐渐增大,并在焊接热源到达其正上方的 50 s 时达到最大,约为 0.44 mm,而焊接板厚 B 为 4.5 mm, U_r/B 小于 0.1,并未达到达到烧穿的临界值,而实际过程中却产生了烧穿,显然使用内部点径向变形值与实际有一定差距。

考察 50 s 时焊接径向变形的瞬时最大值云图,如图 8 所示,发现红色区域表示的径向瞬时最大变形量已经达到了 0.52 mm,这个值与板厚的比值已经大于了 0.1,结论为烧穿,符合实际情况。可见,瞬时径向变形最大值能更好的预测烧穿。

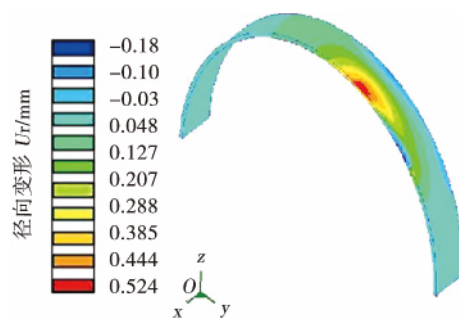


图 8 6 MPa 压力下 50 s 点径向变形场

Fig. 8 Radial direction deformation field of NODE50 with 6 MPa pressure

此外,在按照给定的焊接参数按照 3 mm/s 进行焊接修复,焊接进行到 50 s 时,焊缝长度约为 150

mm,所以在给定的焊接参数、焊接速度以及给定压力条件下进行焊接修复时,焊缝进行到 150 mm 时为烧穿危险点,此工况焊缝应短于 150 mm.

3 结 论

(1) 0~4 MPa 压力范围内进行在役焊接修复时,径向变形量随着压力的增大而逐渐增大,而在 4~6 MPa 压力范围内,径向变形随着压力的增大逐渐减小,并在压力 6 MPa 时近似于常压焊接的变形量.

(2) 在所选取的焊接参数条件下,针对在役焊接接近缝区的一点以及焊接修复 150 s 各时刻的径向变形量进行了研究,结果表明,随着焊接修复时间的增大,径向变形量逐渐增大,具有时间效应.

(3) 径向变形量的时间效应表明,焊接修复不宜采用连续的长焊道,采用短道焊以及断续焊有助于减小烧穿的发生.

(4) 采用径向变形瞬时最大值的预测结果比采用内部点径向变形量的计算结果预测烧穿更接近于实际情况.

参考文献:

- [1] Li Chaowen, Wang Yong, Han Bin, *et al.* Advance of burn-through research on in-service welding of high pressure gas pipelines[J]. Pressure Vessel Technology, 2008, 25(8): 40-45.
- [2] Chen Yuhua, Wang Yong, Han Bin. Metallurgical microstructure and fine structure in local brittle zone of in-service welding of X70 pipeline steel[J]. Transactions of Materials and Heat Treatment, 2007, 28(1): 77-80.
- [3] Bian Yuzhi, Liu Yang, Wang Xinhua. Comparison and analysis on high temperature ductility of X65 and X70 pipeline steel[J]. Journal of Iron and Steel Research, 2007, 19(11): 51-54.
- [4] Otegui J L, Cisilino A, Rivas A, *et al.* Influence of multiple sleeve repairs on the structural integrity of gas pipelines[J]. In-

ternational Journal of Pressure Vessels and Piping, 2002, 79(11): 759-765.

- [5] Guo Guangfei, Wang Yong, Han Tao. Burnthrough failure mechanism of in-service welding of pipeline[J]. Materials Science & Technology, 2012, 20(3): 62-66.
- [6] API 1104. Welding of pipelines and related facilities, appendix B: in-service welding[S]. USA: American Petroleum Institute, 1999.
- [7] Li Peilin, Lu Hao. Sensitivity analysis and prediction of double ellipsoid heat source parameters[J]. Transactions of the China Welding Institution, 2011, 22(1): 85-89.
- [8] 陈玉华,王 勇. 基于 SYSWELD 的运行管道在役焊接热循环数值模拟[J]. 焊接学报, 2007, 28(1): 85-89.
Chen Yuhua, Wang Yong. Numerical simulation of thermal cycle of in-service welding onto active pipeline based on SYSWELD[J]. Transactions of the China Welding Institution, 2007, 28(1): 85-89.
- [9] Ren Ying, Zhang Hong. Heat transfer theory[M]. Dongying: China University of Petroleum Press, 1988.
- [10] Watt D F. An algorithm for modeling microstructure development in weld heat-affected zones (Part A) [J]. Acta Metallurgica, 1988, 36(11): 3029-3035.
- [11] Bang I W, Son Y P, Oh K H, *et al.* Numerical simulation of sleeve repair welding of in-service gas pipelines[J]. Welding Journal, 2002, 81(12): 273-282.
- [12] Wei Liu, Shuang Liu, Junjie Ma, *et al.* Real time monitoring of the laser hot-wire welding process[J]. Optics & Laser Technology, 2014, 57: 66-76.
- [13] 陈玉华,王 勇,何建军. 输气管线在役焊接管道内壁变形的数值模拟[J]. 焊接学报, 2010, 31(1): 110-112.
Chen Yuhua, Wang Yong, He Jianjun. Numerical simulation on deformation in inner pipe wall of in-service welding onto gas pipeline[J]. Transactions of the China Welding Institution, 2010, 31(1): 110-112.

作者简介: 郭广飞,男,1984 年出生,工学博士研究生. 主要从事压力容器与管道安全工程的研究. 发表论文 11 篇. Email: guo6324@163.com

通讯作者: 王 勇,男,教授,博士研究生导师. Email: wangyong@upc.edu.cn

joint was about 70 μm at weld metal (WM) and heat affected zone (HAZ) , about 50 μm at base metal (BM) . The grains of the welded surface were refined in which the grain size of WM surface reached 70-300 nm , and the grain size of BM surface reached 50-500 nm.

Key words: 7A52 aluminum alloy; UIT; microstructure

Study of laser pre-melting activating welding on low carbon steel

YIN Yan¹ , WANG Zhanchong¹ , ZHANG Ruihua² , ZHU Min³ , LUO Xiaojun³ (1. State Key Laboratory of Gansu Advanced Non-ferrous Metal Materials , Lanzhou University of Technology , Lanzhou 730050 , China; 2. China Iron & Steel Research Institute Group , Beijing 100081 , China; 3. The Second Construction Company of CNPC , Lanzhou 730060 , China) . pp 39 - 42

Abstract: The laser pre-melting activating welding of low carbon steel with 8 mm thickness was study. Firstly , the surface of the substrate was pre-melted by the low power laser in oxygen atmosphere to form an oxide layer on the surface. Then TIG welding or laser arc hybrid welding was used to cover the weld. The effect of welding parameters on the weld depth and width was studied. The result shows that the arc was not shrunk during the welding after laser pre-melting. However the penetration increased about 0.5 times. The weld surface had a good appearance. The penetration increased with the increase of arc current , which had more increase after laser surface pre-melting. The increase of welding speed resulted in a decrease of penetration. The penetration increased with the increase of the pre-melting laser power. Simultaneously , the increase of laser power of hybrid welding also can increase the penetration. The oxygen content of the weld increased when the surface of weld was pre-melted by laser , which leads to the temperature coefficient of surface tension gradient changed from a negative value to a positive value. That is the reason why the penetration can be increased after laser pre-melting.

Key words: low carbon steel; activating welding; TIG welding; hybrid welding

In-situ observation on microstructure of Sn-3.0Ag-0.5Cu solder/Cu joint during long-term aging at 110 °C

LI Shuai , YAN Yanfu , ZHAO Yongmeng , WANG Hongna (College of Material Science and Engineering , Henan University of Science and Technology , Luoyang 471003 , China) . pp 43 - 46

Abstract: Based on the home-made in-situ observation device , the microstructure and the growth kinetic of Sn-3.0Ag-0.5Cu solder/Cu joint were investigated under 110 °C thermal exposure condition. The intermetallic compounds (IMCs) presented at interface was thickened with increasing exposure time. At the same time , the growth of IMCs have three-dimensional characteristics. The Cu_6Sn_5 varied evidently in the longitudinal direction with a gradual decrease of height , while it was changed slowly in the transverse direction with the aging time. The SEM shows that the microstructure of IMCs varied from the scallop-shape to a layered structure with stratified phenomenon.

Key words: IMC; microstructure; three-dimensional characteristics; stratified phenomenon

Effect of welding thermal cycle on microstructure and properties of intercritically reheated coarse grained heat affected zone in SA508-3 steel

LÜ Xiaochun^{1,2} , HE Peng¹ , QIN Jian² , DU Bing² , HU Zhongquan³ (1. State Key Laboratory of Advanced Welding and Joining , Harbin Institute of Technology , Harbin 150001 , China; 2. Harbin Welding Institute , Harbin 150028 , China; 3. Mechanical Engineering Department of Tsinghua University , Beijing 100084 , China) . pp 47 - 49

Abstract: The effect of welding thermal cycle on the microstructure and properties of the intercritically reheated coarse grained heat affected zone (IC-CGHAZ) was studied using thermal simulation technology. The results showed that the formation of fine martensite along the prior austenite grain boundaries deteriorating the performance of IC-CGHAZ. The IC-CGHAZ is the weakest area in the welded joint. The impact toughness of the joint was improved significantly allowing the joint have a good match in hardness and toughness when the IC-CGHAZ experienced a thermal cycle with peak temperature of 400 - 650 °C. The microstructure and properties of IC-CGHAZ can be improved effectively by precisely controlling the layer thickness and the welding thermal cycle conditions in SA508-3 steel multi-pass welding processing.

Key words: SA508-3 steel; IC-CGHAZ; peak temperature; welding thermal cycle

Study on simulation of underwater friction stud welding process based on Abaqus

GAO Hui , JIAO Xiangdong , ZHOU Canfeng , LI Guanqun (Research Centre of Energy Engineering Advanced Joining Technology , Beijing Institute of Petrochemical Technology , Beijing 102617 , China) . pp 50 - 54

Abstract: The finite element simulation software Abaqus was used to study the friction stud welding process. A python script based on the Abaqus/stand algorithm has been designed , which can realize the functions of parameterization modeling , automatic remeshing , results mapping , thermal boundary automatic selection and so on. This can effectively solve the difficulty of convergence in calculation that is caused by the large scale non-linear plastic deformation of materials. The simulation results of the plastic deformation of welded stud are basically consisted with and the experimental results effectively proving the validity of the finite element model. In addition , the analysis results of welding stress and temperature fields can explain the difference of the joint quality welded in the air and water with the same welding parameters. These works may have important guiding significance for the underwater friction stud welding application and welding process selection.

Key words: friction stud welding; finite element; nonlinear; Python script; underwater welding

Numerical simulation on radial deformation of in-service welding gas pipeline

GUO Guangfei^{1,2} , WANG Yong² , HAN Tao² (1. National Safety Engineering Technology Research Center for Pressure Vessels and Pipelines of China , General Machinery Research Institute , Hefei 230031 , China; 2. College of Mechanical and Electronic Engineering , China University of Petroleum , Qingdao 266580 , China) . pp 55 - 58

Abstract: The software SYSWELD was used to simulate how the internal pressure and the welding repair time affect the radial direction deformation of pipeline for the in-service welding. The results of simulation was verified by the experiment. When the in-service welding was carried out in the pipeline with an internal pressure range of 0-4 MPa , the radial direction deformation increased with the increase of the pressure. When the internal pressure was in the range of 4-6 MPa , the deformation decreased with the increase of pressure. The deformation at the internal pressure of 6MPa was almost equally as that at that one at normal pressure. When the repair welding process progressed , the amount of deformation was gradually increased. In order to predict the occurrence of burned hole , the utilization of instantaneous radial deformation is better than using the radial deformation of the internal point.

Key words: in-service welding; gas pipeline; radial deformation; numerical simulation

Comparison of Ar-He and Ar-He-N₂ gas shielding metal arc welding technology for aluminum alloy LU Hao¹ , XING Liwei¹ , LIANG Zhimin² (1. CSR Qingdao Sifang CO. ,LTD. , Technique headquarters , Qingdao , 266111 , China; 2. Faculty of Material Science and Engineering , Hebei University of Science & Technology , Shijiazhuang 050000 , China) . pp 59 – 62

Abstract: In order to recognize the importance of the addition of trace nitrogen in the triple gas mixture , the difference of the aluminum welding was studied in terms the arc shape , macro and micro-welded joint structure , the width of heat affected zone , by using pure argon , binary Ar-He mixture , triple Ar-He-N₂. In comparison to the MIG welding using pure argon and Ar-He , the arc was more concentrated that allow a production of best quality of joint with highest impact toughness and narrow HAZ. The performance of the welding joint using pure argon was the next-best. The work shows that adding trace nitrogen is a very important factor for the improvement of welding quality using Ar-He-N₂ triple gas shielding.

Key words: Ar-He; Ar-He-N₂ gas; aluminum

3D numerical simulation on explosive welding of Al/Ti composite tube DENG Wei^{1,2} , LU Ming² , TIAN Xiaojie³ (1. 63981 Unite of PLA , Wuhan 430311 , China; 2. College of Field Engineering , PLA Univ. of Sci. & Tech. , Nanjing 210007 , China; 3. College of Engineering , China University of Ocean , Qindao 266100 , China) . pp 63 – 66

Abstract: The different explosive welding process of composite tube welding induces a different progress in welding process compared to the composite plate welding. The relatively confined space of the composite tube lead to difficulties in the observation of the welding process. This paper simulate the explosive welding process of composite tube through software AUTODYN. On the basis of the verification of the model , the formation of the jet and the unique structure of waveform interface were analyzed. The jet induced wavy bonding satisfies the penetrating mechanism hypothesis. The simulation results are in good agreement with the experimental results , which provide important information for the further study on the wave structure and jet for-

mation mechanism of explosive welding.

Key words: explosive welding; jet; composite tube; interfacial wave

Research on resistance welding of DZ-47 electrical contact

ZHU Shiliang¹ , ZHANG Zhongdian¹ , TIAN Xiubo¹ , WU Laijun¹ , QI Songyu² (1. State Key Lab of Advanced Welding and Joining , Harbin Institute of Technology , Harbin 150001 , China; 2. Technical Department of FAW Car Co. , Ltd. , Changchun 130012 , China) . pp 67 – 71

Abstract: Electrical contact is the execution unit of low-voltage electrical equipment. The welding quality directly determines the service life and reliability of entire electrical equipment. In this paper , resistance welding was used in the welding of DZ-47 electrical contact. The influence of welding current , welding time and electrode pressure on the shear stress of the contact was analyzed. The welding interface morphology and elemental distribution were also studied. The results show that resistance welding is feasible for electrical contact welding under the appropriate processing parameters. It is additionally found that in the case of same process parameters the interface diffusion layer thickness and the amount of diffusion of elements are not the same due to the electromagnetic force and the unreasonable design of electrical contact.

Key words: electrical contact; resistance welding; morphology; element distribution

Analysis of quality characteristics information of aluminum resistance spot welding joint FENG Linjiang^{1,2} , JI Chuntao³ , YI Runhua³ , WANG Hua^{1,2} , CHEN Jie^{1,2} , ZHANG Zuli^{1,2} , LUO Song^{1,2} (1. National Engineering Research Center for Instrument Functional Materials , Chongqing 400707 , China; 2. Chongqing Materials Research Institute , Chongqing 400707 , China; 3. Nanchang Hangkong University , Nanchang 330063 , China) . pp 72 – 76

Abstract: In order to study the quality of resistance spot welding joint , three groups of dynamic data were analyzed and drew to curve during the resistance spot welding of aluminum alloy 2A12 , namely , the electrode force , the electrode displacement and welding current. The results show that the change tendency of the electrode force was depressing slightly at the beginning of the welding , then a small increase with slight fluctuations , and finally a downward-sloping trend. Unqualified weld was formed when the force is under or over the normal stress at each stage. The rising rate of the displacement curve is related to the welding current and the energy efficiency. The shape of the displacement curve between the maximum displacement and the loading forging force is related to the amount of melting metal and the size of the softening zone.

Key words: quality of spot welding; electrode displacement; electrode force; welding current

In-situ synthesis of TiN coating prepared by laser cladding

ZHAO Jian¹ , HE Wenxiong² , LÜ Zhijun³ , ZHAO Hongyun² (1. State Key Laboratory of Advanced Welding and Joining , Harbin Institute of Technology , harbin 150001 , China;